

In-situ hybridization strategy construct heterogeneous interfaces to form electronically modulated MoS₂/FeS₂ as the anode for high performance lithium-ion storage

Dazhi Li¹, Changlong Sun¹, Zeqing Miao², Kesheng Gao³, Zeyang Li¹, Wei Sun¹, Shengjing Guan⁴, Xiaofei Qu^{1*} and Zhenjiang Li^{1*}

¹ *College of Materials Science and Engineering, Qingdao University of Science and Technology, Qingdao 266042, Shandong, P. R. China*

² *College of Electromechanical Engineering, Qingdao University of Science and Technology, Qingdao 266061, Shandong, P. R. China*

³ *Songshan Lake Materials Laboratory, Dongguan 523808, Guangdong, China*

⁴ *School of Chemistry and Chemical Engineering, Shandong University of Technology, Zibo 255049, Shandong, China*

*E-mail address:

zhenjiangli@qust.edu.cn (Zhenjiang Li)

quxiaofei@qust.edu.cn (Xiaofei Qu)

Contents:

S1. Characterization methods and details analysis

S2. Results and discussion

Figure S1. SEM of MoS₂/FeS₂ *ex-situ* growth mechanism.

Figure S2. SEM of pure (a-b) MoS₂ and (c-d) FeS₂.

Figure S3. Selected Area Electron Diffraction (SAED) of MoS₂/FeS₂.

Figure S4 Galvanostatic charge-discharge (GCD) curves of pure MoS₂ and FeS₂ at 0.1 A g⁻¹.

Figure S5. Capacity retention of pure MoS₂ and FeS₂ at 0.1 A g⁻¹.

Figure S6. Capacity retention of pure MoS₂ and FeS₂ at 1.0 A g⁻¹.

Figure S7. EIS of MoS₂/FeS₂, pure MoS₂ and FeS₂.

S1. Characterization methods and details analysis

1.1. Materials characterization

The structure and morphology of MoS₂/FeS₂ were characterized by scanning electron microscopy (SEM, Hitachi S-4800). The EDX elemental spectroscopy of pristine MoS₂/FeS₂ was observed using a Talos TEM (FEI, Talos F200X). The powder X-ray diffraction (XRD) measurements were performed on a Rigaku D/MAXRB diffractometer from 5° to 80° (Philips, X'pert Pro MPD, Netherlands), and the excitation wavelength is Cu *K*α radiation ($\lambda = 0.15$ nm). Transmission electron microscopy (TEM) and corresponding high-resolution images were obtained using a Philips Tecnai 20U-Twin microscope at an acceleration voltage of 200 kV. The binding energies of the MoS₂/FeS₂ nanoparticles were acquired by X-ray photoelectron spectroscopy (XPS) on the Thermo ESCALAB 250 with Al *K*α radiation (1486.8 eV) as the excitation source. The data fitting was conducted using XPSPEAK 4.1 software. All the XPS spectra were calibrated with the binding energy of C 1s electron at 284.8 eV.

1.2. Device assembly measurements

CR2032-type coin cells were used to investigate the electrochemical performance of MoS₂/FeS₂, pure MoS₂ and FeS₂. The concentration of moisture and oxygen of argon filled glove box are both below 1 ppm. 80 wt% active materials, 10 wt% conductive carbon (ketjen black), and 10 wt% polyvinylidene fluoride (PVDF) as the binder was mixed in N-methyl-2-pyrrolidone, then the mixture was pasted on copper foil and dried at 80 °C. The average loading density of these active materials is 2.0 mg. Li metal is used as both the counter and reference electrodes. Li metal cathode and MoS₂/FeS₂, pure MoS₂ and FeS₂ anodes were electronically separated by a polypropylene film (Celgard 2320) saturated with electrolyte. The electrolyte solution is consist of LiPF₆ (1 M) in ethylene carbonate/dimethyl carbonate/diethy carbonate (1:1:1 vol%). Neware CT-3008W system (Neware Technology Ltd., P. R. China) is used to carry out galvanostatic charge and discharge tests at various current densities. The cell was

discharged at 0.5 A g^{-1} for 5 min, followed by a 20 min relaxing from 0.01 to 3.0 V (Shanghai CH Instruments Co., China). Electrochemical impedance spectroscopy (EIS) test is also recorded by CHI660E electrochemical workstation with the frequency ranging from 0.01 Hz to 1 MHz at a 5 mV amplitude signal without applied voltage bias.

S2. Results and discussion

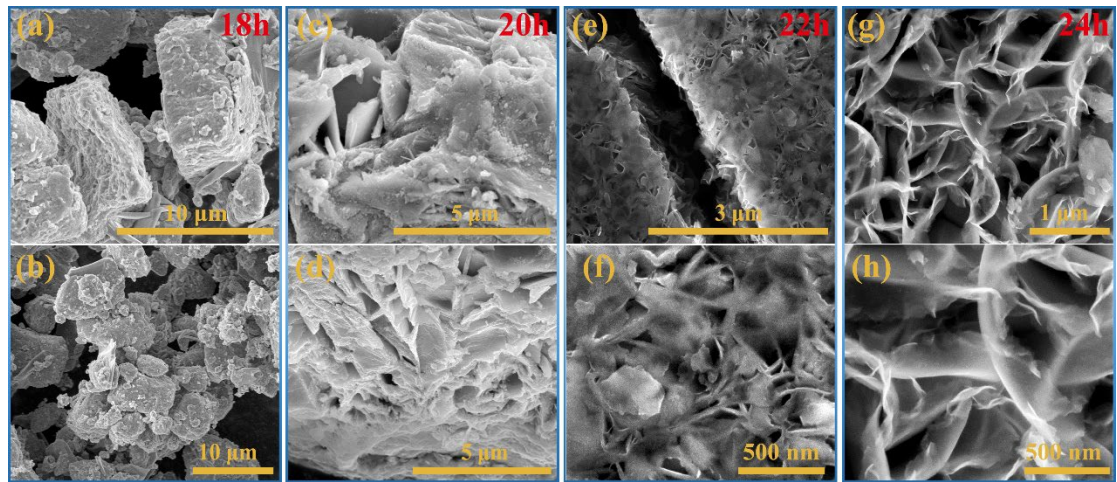


Figure S1. SEM of MoS₂/FeS₂ *ex-situ* growth mechanism.

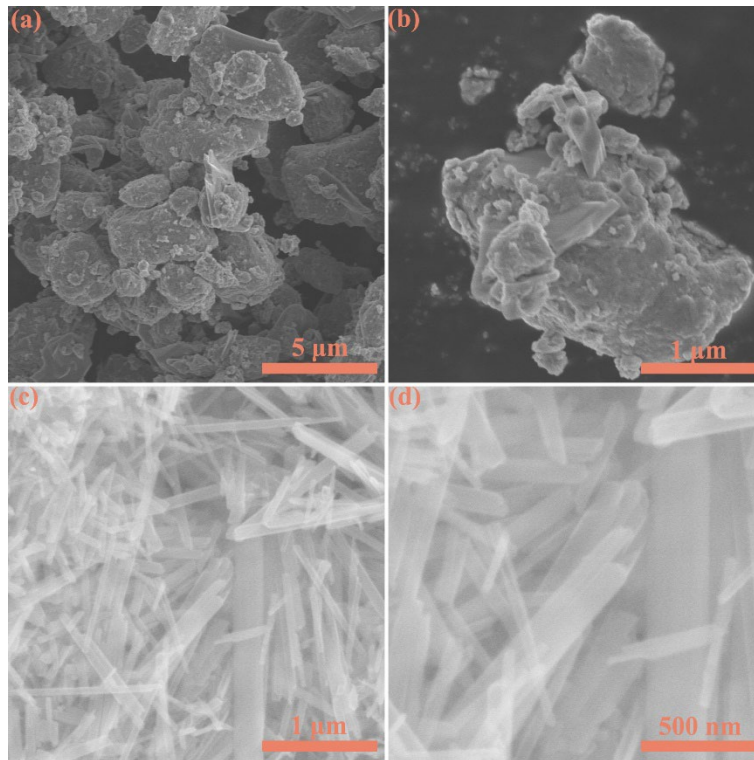


Figure S2. SEM of pure (a-b) MoS₂ and (c-d) FeS₂.

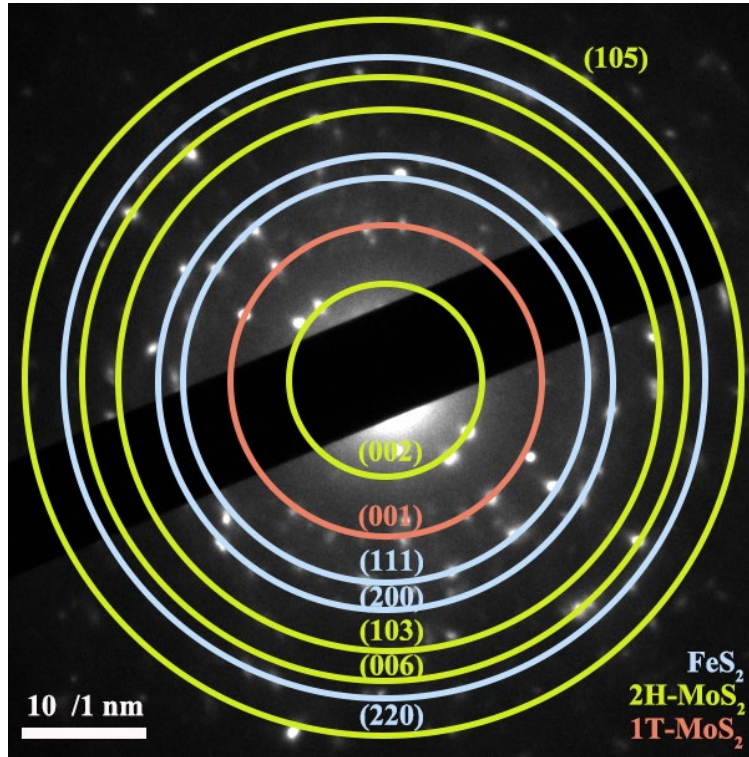


Figure S3. Selected Area Electron Diffraction (SAED) of MoS₂/FeS₂.

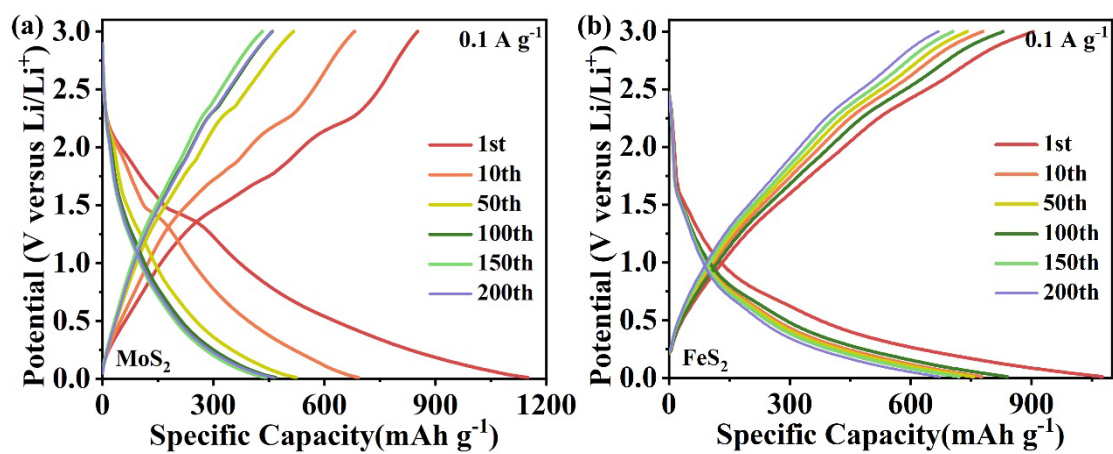


Figure S4 Galvanostatic charge-discharge (GCD) curves of pure MoS₂ and FeS₂ at 0.1 A g⁻¹.

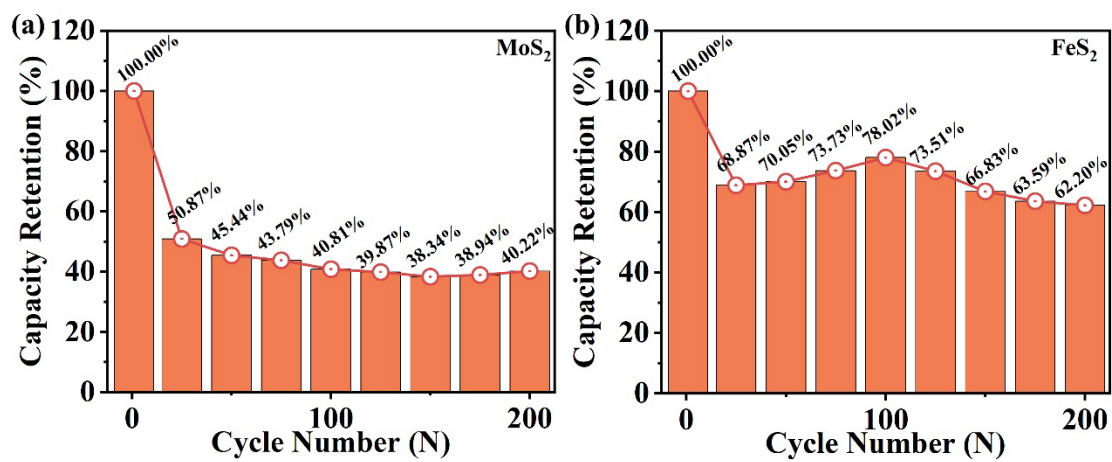


Figure S5. Capacity retention of pure MoS₂ and FeS₂ at 0.1 A g⁻¹.

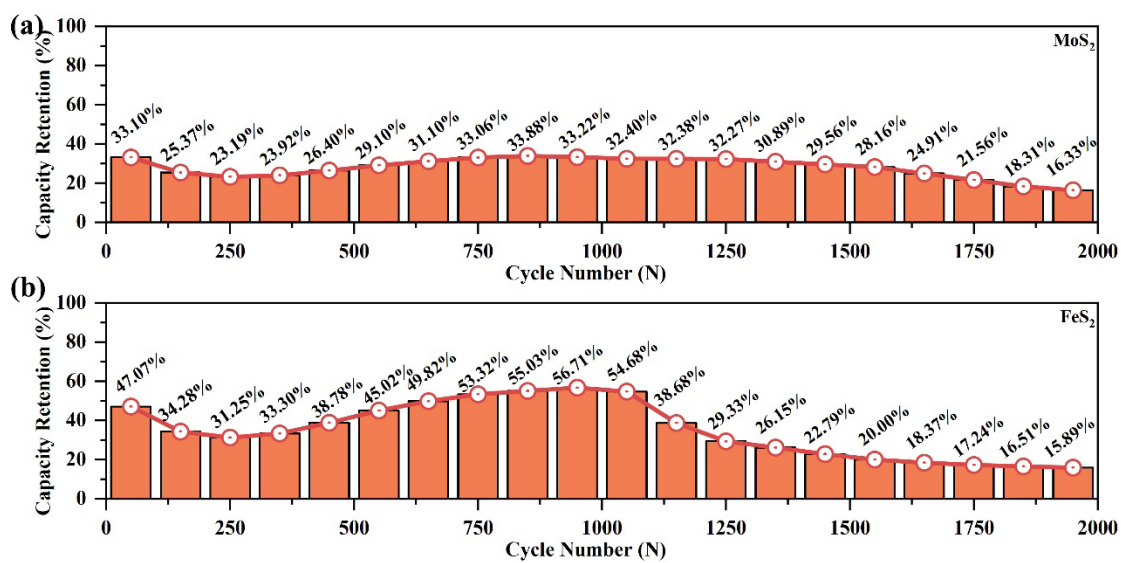


Figure S6. Capacity retention of pure MoS₂ and FeS₂ at 1.0 A g⁻¹.

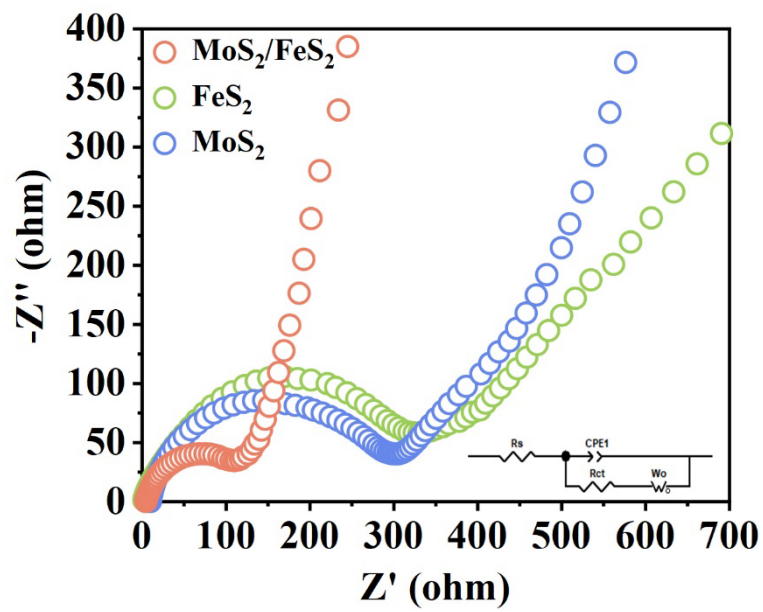


Figure S7. EIS of $\text{MoS}_2/\text{FeS}_2$, pure MoS_2 and FeS_2 .